

2



AD-A277 062



DEPARTMENT OF DEFENCE
DEFENCE SCIENCE AND TECHNOLOGY ORGANISATION
AERONAUTICAL RESEARCH LABORATORY

MELBOURNE, VICTORIA

Technical Note 63

**FINITE ELEMENT ANALYSIS OF MB326H MACCHI WING LOWER
SPAR CAP FATIGUE CRACKS**

by

D. REES

DTIC
ELECTE
MAR 18 1994
S E D

94-08748



3096

Approved for public release

© COMMONWEALTH OF AUSTRALIA 1993

DECEMBER 1993

94 3 18 008

This work is copyright. Apart from any use as permitted under the Copyright Act 1968, no part may be reproduced by any process without prior written permission from the Australian Government Publishing Services. Requests and enquiries concerning reproduction and rights should be addressed to the Manager, Commonwealth Information Services, Australian Government Publishing Services, GPO Box 84, Canberra ACT 2601.

THE UNITED STATES NATIONAL
TECHNICAL INFORMATION SERVICE
IS AUTHORISED TO
REPRODUCE AND SELL THIS REPORT

DISCLAIMER NOTICE



THIS DOCUMENT IS BEST QUALITY AVAILABLE. THE COPY FURNISHED TO DTIC CONTAINED A SIGNIFICANT NUMBER OF COLOR PAGES WHICH DO NOT REPRODUCE LEGIBLY ON BLACK AND WHITE MICROFICHE.

**DEPARTMENT OF DEFENCE
DEFENCE SCIENCE AND TECHNOLOGY ORGANISATION
AERONAUTICAL RESEARCH LABORATORY**

Technical Note 63

**FINITE ELEMENT ANALYSIS OF MB326H MACCHI WING LOWER
SPAR CAP FATIGUE CRACKS**

by

D. REES

SUMMARY

A three dimensional finite element analysis of cracks in the MB326H Macchi wing lower spar cap is presented. The case of cracks emanating from the intersection of a wing attachment fitting bolt hole and a web attachment fastener hole at wing station Y900 is considered. Stress intensity factors for two proposed crack geometries and the residual strength of the ligament above the web attachment fastener hole in the spar cap flange are calculated.



© COMMONWEALTH OF AUSTRALIA 1993

POSTAL ADDRESS: Director, Aeronautical Research Laboratory
506 Lorimer Street, Fishermens Bend
Victoria 3207, Australia.

TABLE OF CONTENTS

	Page Nos.
1. INTRODUCTION	1
2. FINITE ELEMENT MODEL	1
3. CALCULATION OF STRESS INTENSITY FACTORS.....	2
4. RESULTS.....	3
4.1 Uncracked Model.....	3
4.2 Crack Case 1.....	3
4.3 Crack Case 2.....	4
5. PLASTIC ANALYSIS.....	4
6. DISCUSSION.....	5
7. CONCLUSION.....	5

REFERENCES

TABLES 1-3

FIGURES 1-17

DISTRIBUTION

DOCUMENT CONTROL DATA

Accession For	
NTIS CRA&J	<input checked="" type="checkbox"/>
DTIC TAB	<input type="checkbox"/>
Unannounced	<input type="checkbox"/>
Justification	
By	
Distribution /	
Availability Codes	
Dist	Avail and/or Special
A-1	

1. INTRODUCTION

The wing lower spar cap of the Macchi MB326H is susceptible to fatigue cracking at wing station Y910, near the end of the wing attachment fitting (WAF). A life assessment of the spar cap was completed in April 1992 [1]. This was concerned primarily with cracks emanating from a web attachment fastener hole located in the flange of the spar cap.

Following the repair of several wing lower spar caps it became apparent that some of the blind web attachment holes in the base of the spar cap ended in close proximity to WAF bolt holes and that this may influence the fatigue life of the spars. Although no crack growth from these nearly-intersecting holes has been observed, it was considered that further investigation into the problem was appropriate given the history of fatigue cracking in the spar cap and the difficulty of inspection. An alternative crack growth scenario was postulated, see [2], which involved cracks initiating from the intersection of a WAF bolt hole and a web attachment fastener hole. It was also postulated that such cracking may cause failure in the ligament above the web attachment fastener hole in the spar cap flange and that this may be used as a basis for inspection.

It was recognised, however, that it may also be possible for cracks growing from intersecting holes to progress to failure of the section prior to failure of the adjacent uncracked flange hole ligament. In this case, flange surface NDI would detect no flange hole cracking and would provide no assurance of structural safety. To check this possibility, two intersecting hole crack cases (with no spar flange cracking) were investigated, the residual strengths of the cracked regions being compared with that of the (intact) flange hole ligament. The site likely to fail first could thus be ascertained.

A three-dimensional finite element analysis of the lower spar cap and WAF assembly between wing stations Y884 and Y920 was undertaken. The residual strength was determined for the uncracked structure and for the structure containing assumed crack geometries of two sizes.

2. FINITE ELEMENT MODEL

The end of the lower spar cap and wing attachment fitting assembly between wing stations Y884 and Y920 was modelled. This included the last three WAF bolts, see Figure 1. The web attachment fastener holes (Deutsch fasteners) D15 and B16 are adjacent to WAF bolt hole C7. The exact locations and depths of the web attachment fastener holes vary and in some wings B16 nearly intersects with C7. For the purpose of this analysis the centre lines of holes C7, A7, B16 and D15 were modelled as being coplanar, with B16 intersecting C7. The model dimensions are shown in Figure 2.

As well as the uncracked structure, two crack cases were analysed. In both cases a pair of cracks which initiated at the intersection of holes B16 and C7 and propagated

above and below B16 were modelled. For case 1 the crack length is 10mm with circular crack fronts above and below hole B16. For case 2 the crack has propagated along the full length of B16 (13.5mm) with a circular crack front below and a horizontal crack tip at the base of the spar cap flange. The crack geometries are shown in Figure 3.

The analysis was performed using the PAFEC level 6.2 finite element analysis program and run on a Hewlett-Packard 9000 model 750 workstation. Three dimensional, twenty-noded isoparametric brick elements and fifteen-noded isoparametric wedge elements were used. The aluminium alloy spar cap and steel wing attachment fitting were modelled separately. The bolted joint was approximated by modelling the steel WAF bolts so that the bolt mesh shared nodes with the inboard side of the spar cap holes and the outboard side of the WAF holes. The F.E. mesh is shown in Figure 4. It contains 2764 elements and 37980 degrees of freedom. A linear elastic analysis was performed in each case.

Nodes in the x-y plane were restrained in the z-direction at Y884. This included both the spar cap and WAF and is not strictly consistent with the actual deformation in a bolted joint. The effect of this restraint was to underestimate the load transfer into the WAF resulting in higher spar cap stresses. This is conservative for this analysis. Despite this, the modelling of the WAF and bolts should produce a realistic stress concentration in the WAF bolt holes. Nodes in the z-x plane at y=0 were restrained in the y-direction, see Figure 4. This provides a bending restraint which is consistent with a full scale fatigue test [3] in which equal strains were measured at the top and bottom of the spar cap.

A uniform tensile pressure load of 14.5 MPa was applied to the spar cap cross-section at Y920, see [3,4]. This corresponds to the +1g normal load factor.

The spar cap material is Al 7075, with $E = 71000MPa$, $\nu = 0.33$, $F_{tu} = 530MPa$, $F_{ty} = 454MPa$ and $K_{Ic} = 32.6MPa\sqrt{m}$. The WAF and bolts are steel with $E = 210000MPa$ and $\nu = 0.3$.

3. CALCULATION OF STRESS INTENSITY FACTORS

The stress intensity factor was calculated at various locations around the crack front from the FE displacement solutions using equation 1.

$$K_I = \frac{uE}{4(1-\nu^2)}\sqrt{\frac{2\pi}{l}} \quad (1)$$

where u is the mode 1 nodal displacement near the crack tip, E is the elastic modulus, ν is Poisson's ratio and l is the distance from the node to the crack tip [5].

4. RESULTS

4.1 Uncracked Model

A section of the F.E. mesh through the intersecting holes for the uncracked case is shown in Figure 5. For this section the net section stress is equal to 20.2 MPa/g. The maximum principal stress solution is shown in Figure 6. The maximum principal stress in hole D15 is 52 MPa which corresponds to a net section stress concentration factor of 2.6. For WAF bolt hole A7 the maximum stress is 39 MPa giving a stress concentration factor of 1.9, and for the intersection of B16 and C7 the maximum stress is 73 MPa which corresponds to a stress concentration factor of 3.5. These results are summarised in Table 1.

The residual strength of the ligament above D15 may be estimated by calculating the point at which the von Mises equivalent stress, (σ_e), reaches the ultimate tensile stress of the material. However, a significant amount of ductile yielding would be expected at the stress concentration prior to actual failure. A linear elastic analysis is therefore conservative. For the uncracked case the peak von Mises stress in the ligament is 40 MPa/g. The average von Mises stress in the ligament is 22.4 MPa. The residual strength, $F_{tu}/(\sigma_e/g)$, of the ligament is 13.2g.

The maximum von Mises stress at the intersection of B16 and C7 is 60MPa/g which corresponds to a residual strength of 8.8g.

4.2 Crack Case 1

The solution for maximum principal stress for crack case 1 is shown in Figure 7. Note that the stresses for the elements adjacent to the crack tip are not shown. The displaced mesh (highly exaggerated) is shown in Figure 8.

The maximum von Mises stress in the ligament above hole D15 has increased to 60.8 MPa/g, giving a ligament residual strength, $F_{tu}/(\sigma_e/g)$, of 8.7g. The average ligament von Mises stress is 26.6 MPa/g.

For the crack front above hole B16, the stress intensity factor varies from a maximum at the top of $3.69 \text{ MPa}\sqrt{\text{m}}/\text{g}$ to a minimum of $2.48 \text{ MPa}\sqrt{\text{m}}/\text{g}$ near the centre, see Figure 9. The average value of K_I for the upper crack is $2.8 \text{ MPa}\sqrt{\text{m}}/\text{g}$. For the crack front below B16 the stress intensity factor varies from a maximum of $3.37 \text{ MPa}\sqrt{\text{m}}/\text{g}$ at the top to $2.1 \text{ MPa}\sqrt{\text{m}}/\text{g}$ at the bottom. The average is $2.3 \text{ MPa}\sqrt{\text{m}}/\text{g}$. The residual strength, $K_{IC}/(K_I/g)$, based on average and maximum stress intensity factors are 11.6g and 8.8g respectively.

4.3 Crack Case 2

A section through the F.E. mesh for crack case 2 is shown in Figure 10. The solution for maximum principal stress is shown in Figure 11 and the displaced mesh is shown in Figure 12. The maximum von Mises stress in the ligament above hole D15 is 78.7 MPa/g, giving a residual strength, $F_{tu}/(\sigma_e/g)$, of 6.7g. The average ligament von Mises stress is 32.3 MPa/g.

For the upper crack front the stress intensity factor varies from a maximum of 3.38 $MPa\sqrt{m}/g$ in the centre to 3.10 $MPa\sqrt{m}/g$ at the ends. The average value is 3.25 $MPa\sqrt{m}/g$. In the lower crack front the stress intensity varies from a maximum of 4.9 $MPa\sqrt{m}/g$ at the top edge to a minimum of 2.52 $MPa\sqrt{m}/g$ at the centre. The average stress intensity is 3.06 $MPa\sqrt{m}/g$, see Figure 13. The residual strength, $K_{Ic}/(K_I/g)$, for average and maximum stress intensity factors are 10.0g and 6.7g respectively.

The results for crack cases 1 and 2 are presented in Table 2.

5 PLASTIC ANALYSIS

The linear elastic analysis predicted a peak stress at hole D15 much greater than the average ligament stress, indicating that the stress concentration is very localised. A significant amount of plastic yielding and associated stress redistribution would occur before tensile failure of the ligament. To predict accurately the point at which the von Mises stress reaches the material ultimate tensile stress it is necessary to account for this material non-linearity.

A plastic analysis of the structure around hole D15 was therefore performed. For each of the linear elastic models of the spar cap, the elements in the spar cap flange around hole D15 were extracted and the mesh around the hole refined, see Figure 14. The nodal displacements from the linear elastic solutions were applied around the boundary. This modelling strategy is valid provided the influence of the localised yielding is small at the model boundary. The tensile stress-strain curve for aluminium alloy 7075 [6] was approximated by a series of straight lines as shown in Figure 15.

The non-linear solution was run using 0.5g increments and the load required to reach material failure determined. This was defined as the point at which the maximum von Mises stress equalled the material ultimate tensile stress.

The von Mises stress solution for the uncracked case is shown in Figure 16. The plastic region is small, extending over about 20 percent of the ligament. The use of linear elastic displacements at the boundary is therefore a reasonable approximation.

The ligament residual strength results are listed in Table 3. Three definitions of failure are compared. In the first definition, failure occurs when the average ligament stress equals the material yield stress. In the other two definitions the ligament

is deemed to have failed when the maximum von Mises stress reaches the material ultimate stress, one for the linear elastic solution and the other for the plastic solution.

6. DISCUSSION

For the uncracked structure the highest stress lies at the intersection of holes B16 and C7 and corresponds to a stress concentration factor of 3.5. The intersection point is therefore a possible location for crack initiation.

For crack case 1 the upper crack front geometry appears to be realistic since the values of stress intensity are similar at each end. The variation of K_I around the crack front is consistent with the solution for a quarter-circular crack in a square bar, see [7]. For the lower crack front the value of K_I at the top is significantly higher than at the bottom. This is due to the stress concentration at hole B16. Crack growth is therefore likely to propagate faster along B16 and result in a more elliptical crack front. The maximum value of K_I reaches the critical value at 8.8g (lower crack) and the average K_I becomes critical at 11.6g (upper crack).

For crack case 2 the maximum stress intensity factors have increased to give a residual strength of 10.0g (lower crack) and the average value results in a residual strength of 6.7g (upper crack).

Residual strength versus crack length curves for fracture of the proposed cracks and for tensile failure of the ligament above D15 are shown in Figure 17. There was a significant variation of the stress intensity factor along the crack fronts, so results based on both the maximum and average stress intensity factors are included. Only the ligament residual strength based on the plastic analysis is included since the linear elastic result was considered too conservative for the purpose of this analysis.

The residual strength of the spar cap, based on the maximum stress intensity factor, is below the residual strength of the ligament and falls below the limit load of 8g for a crack length of 11.3 mm. For comparison, the residual strength based on the average stress intensity factor lies above the ligament residual strength. There is, therefore, some uncertainty in predicting the load at which fracture would occur. However, these results do indicate that failure could occur from the cracked region in the presence of an intact flange hole ligament: in-service NDI monitoring of the flange surface above the ligament cannot, therefore, guarantee the structural integrity of the section.

7. CONCLUSIONS

1. The analysis indicates that failure of a cracked section could occur with an intact ligament.
2. NDI of the spar cap flange cannot guarantee the structural integrity of the section.

REFERENCES

1. Jost, G.S., Macchi lower wing spar: safe life, ARL Letter Report, 22 April 1992.
2. Barter S.A., Goldsmith N.T., Preliminary report - estimation of the crack growth rate of Macchi wing spar boom WAF bolt hole fatigue cracks. ARL Defect Assessment and Failure Analysis Report No. M7/93, April 1993.
3. Woodbury, S.P., Macchi MB326 fatigue test - test conditions and results, ARL STRUCTURES REPORT 362, May 1976.
4. Piperias, P. & Heller, M., Stress intensity and residual strength for section Y910 of the Macchi MB326H lower spar boom. ARL STRUCTURES TECHNICAL MEMORANDUM 559, 1992.
5. Liebowitz, H., (Ed.), Fracture: An Advanced Treatise, Vols I-IV, Academic Press, New York, 1968.
6. Weiss, V., (Ed.), Aerospace Structural Metals Handbook, Vol II, Non-ferrous Alloys, Syracuse University Press, March 1963.
7. Rooke, D.P. & Cartwright, D.J., Stress Intensity Factors. Her Majesties Stationary Office, London, 1976.

Table 1. Stress concentration factors, K_t , for the uncracked structure

Location	Max. Principal Stress (MPa)	K_t
Upper web fastener hole D15	52	2.6
WAF bolt hole A7	39	1.9
Intersection of holes B16 and C7	70	3.5

Table 2. Stress Intensity Factors, K_I ($\text{MPa}\sqrt{m}/g$)

Crack case	Upper crack		Lower crack	
	Maximum	Average	Maximum	Average
1	3.7	2.8	3.4	2.3
2	3.4	3.3	4.9	3.1

Table 3. Ligament residual strength (g)

Case	Average Ligament	Material Ultimate	Material Ultimate
	Yield	Stress - Linear	Stress - Plastic
uncracked	20.1	13.3	17.0
crack case 1	16.9	8.7	10.6
crack case 2	13.9	6.7	8.8

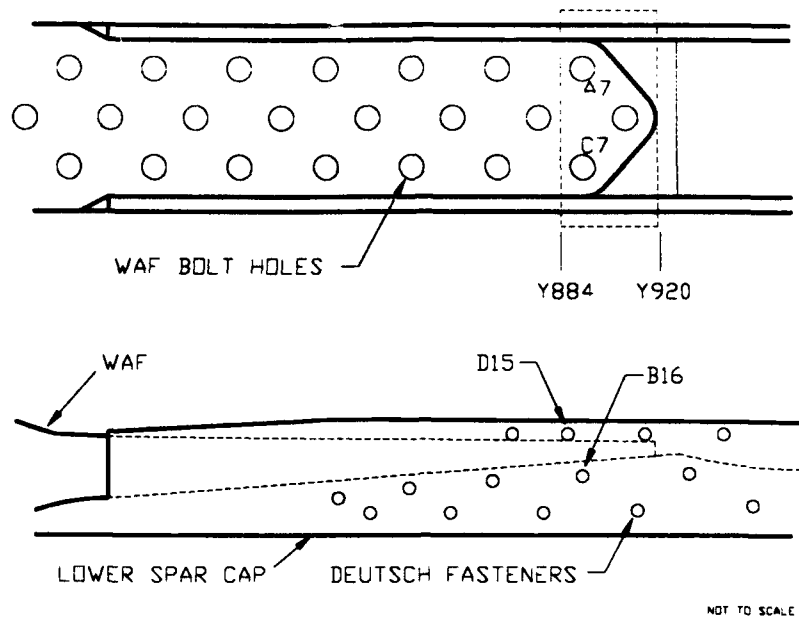


Figure 1 Lower spar cap and WAF assembly

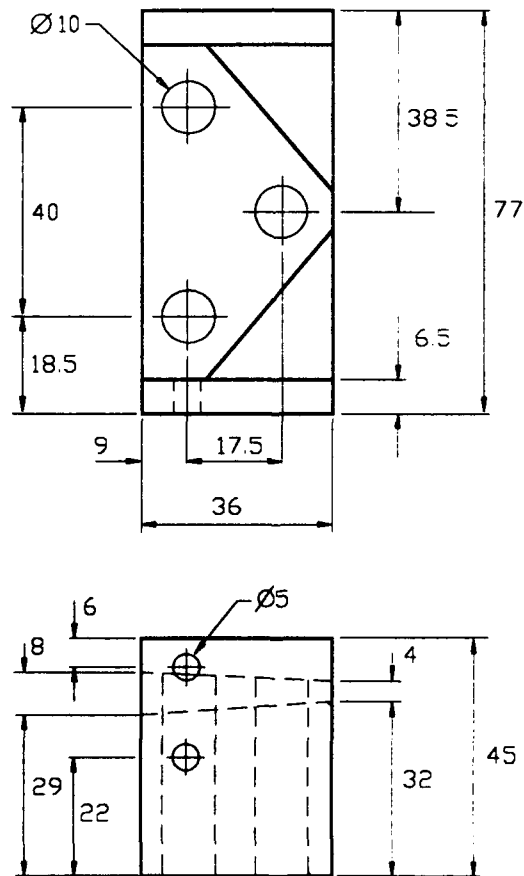
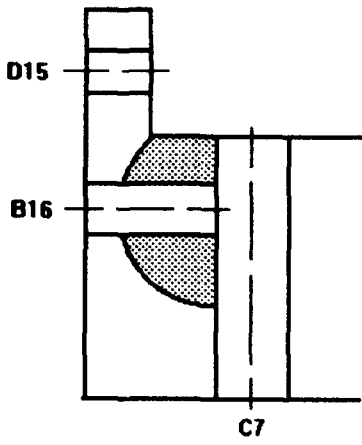
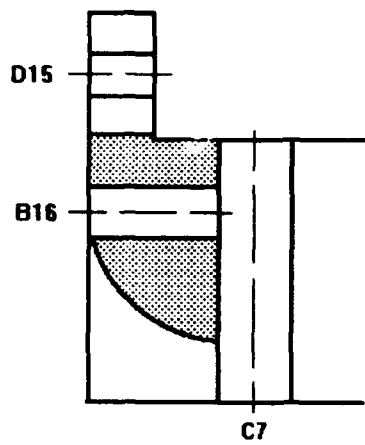


Figure 2 F.E. Model Dimensions



Crack case 1



Crack case 2

Figure 3 Crack case geometries

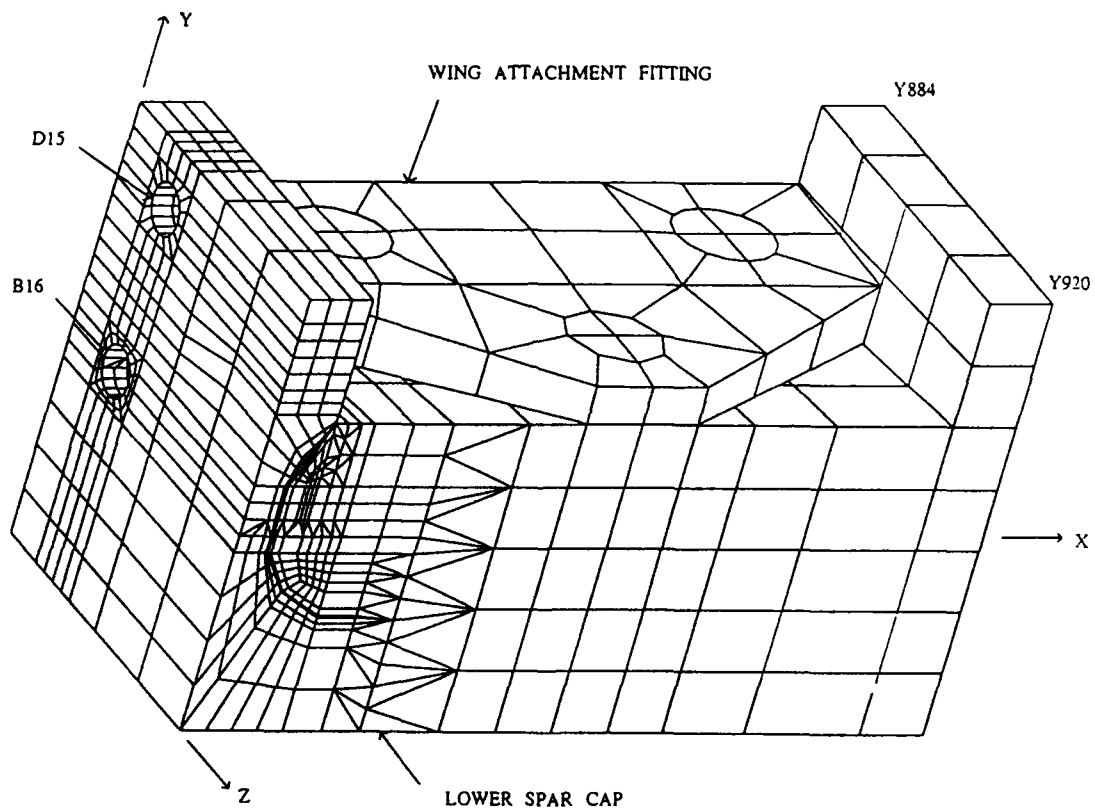


Figure 4 Three dimensional F.E. Mesh

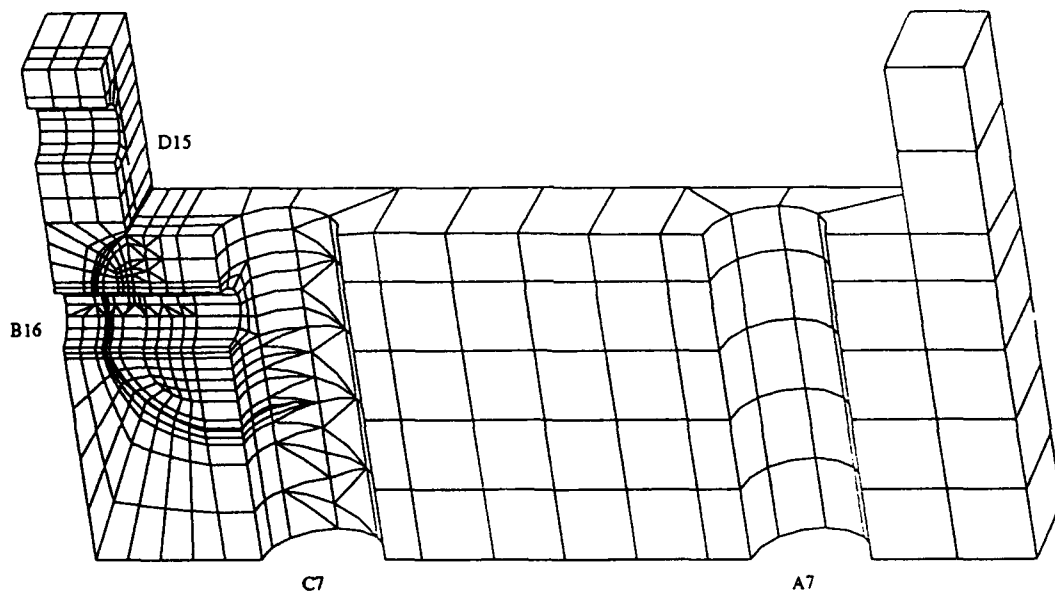


Figure 5 Section through intersecting hole centre lines

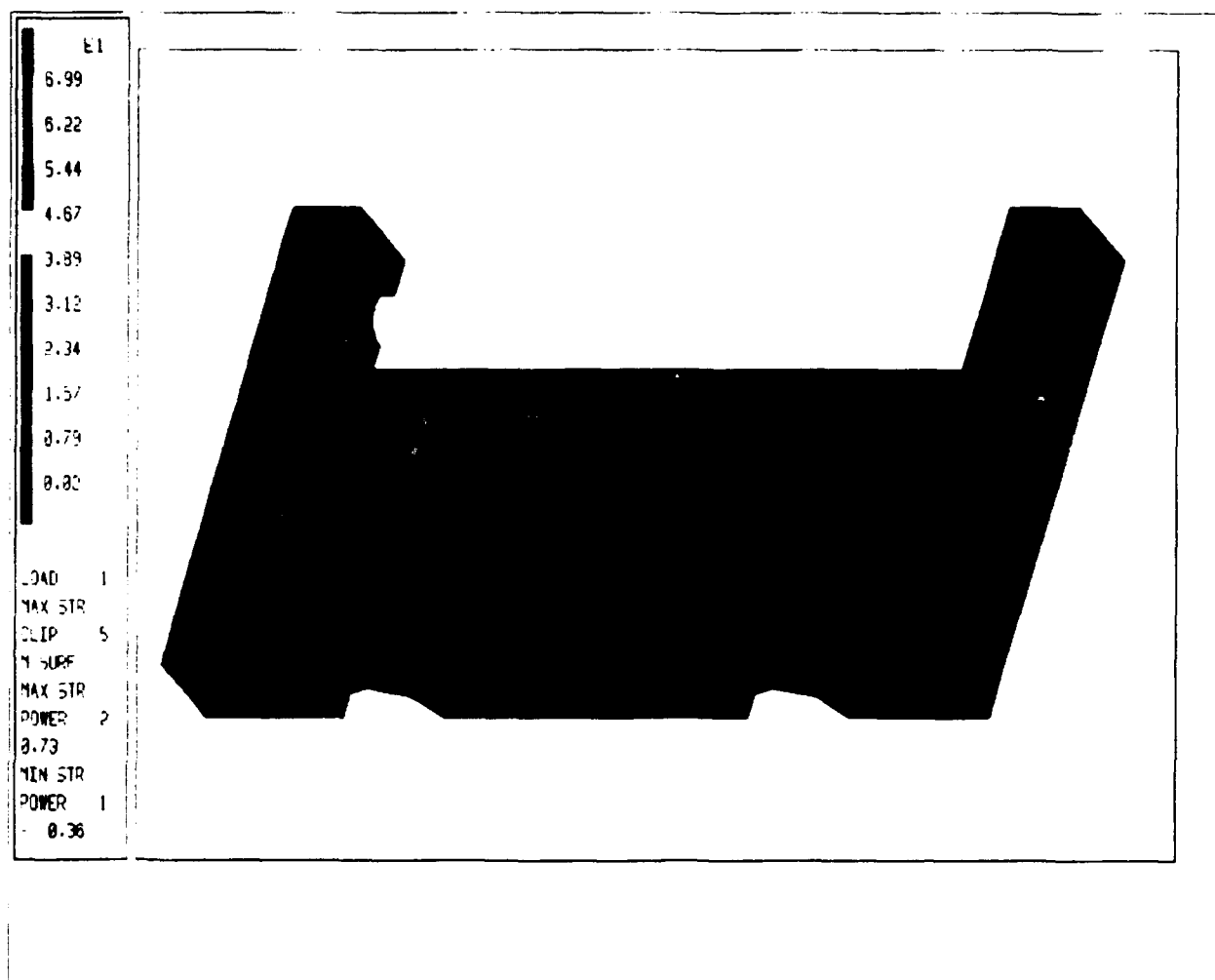


Figure 6 Maximum principal stress solution for the uncracked structure

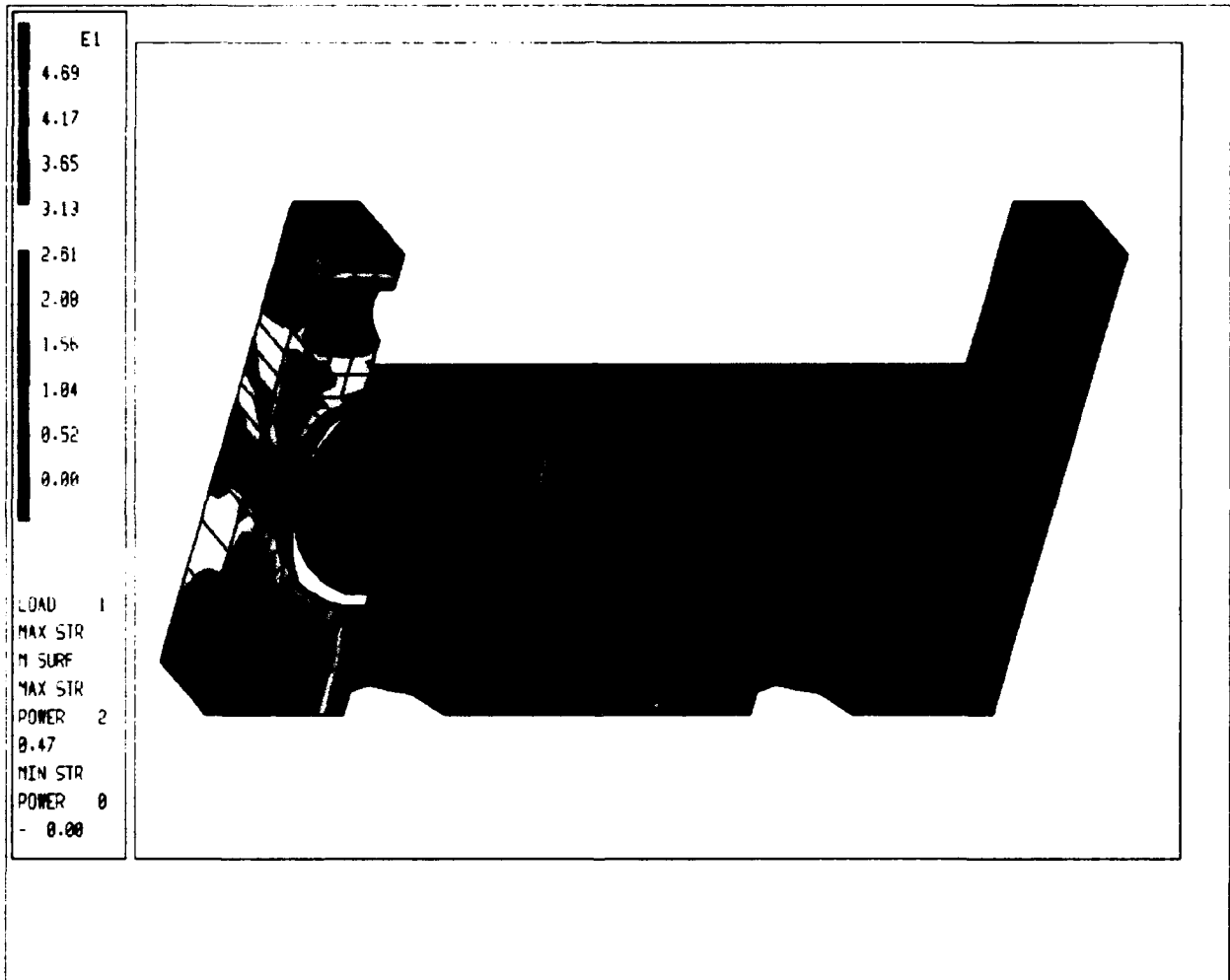


Figure 7 Maximum principal stress solution for crack case 1

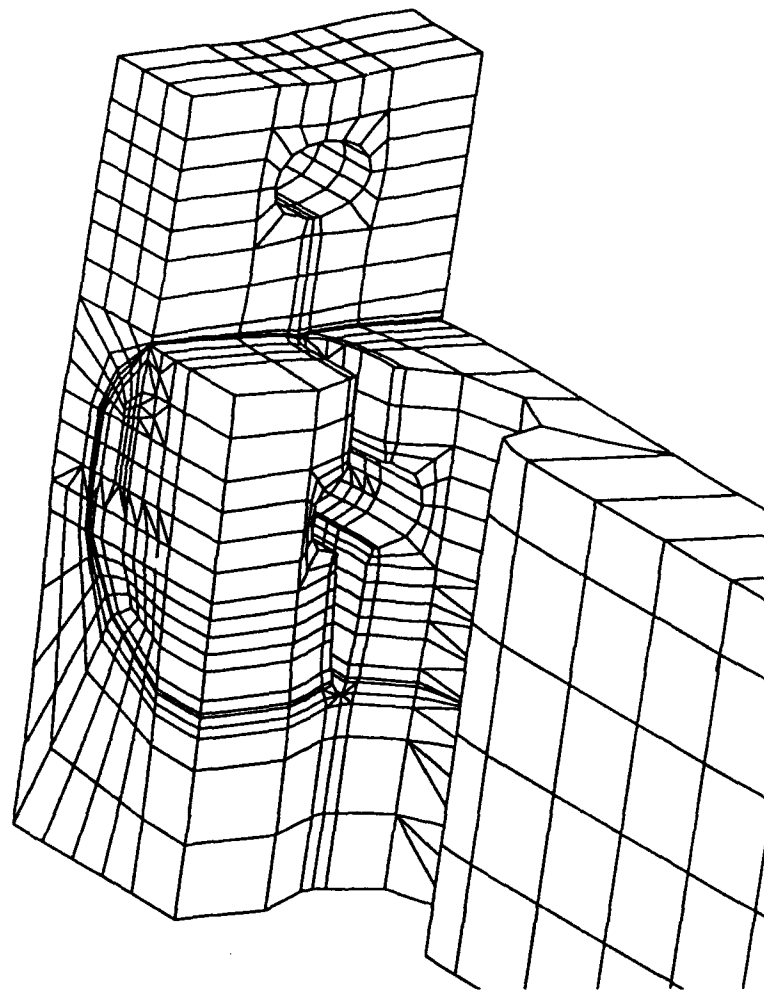


Figure 8 Displaced mesh for crack case 1

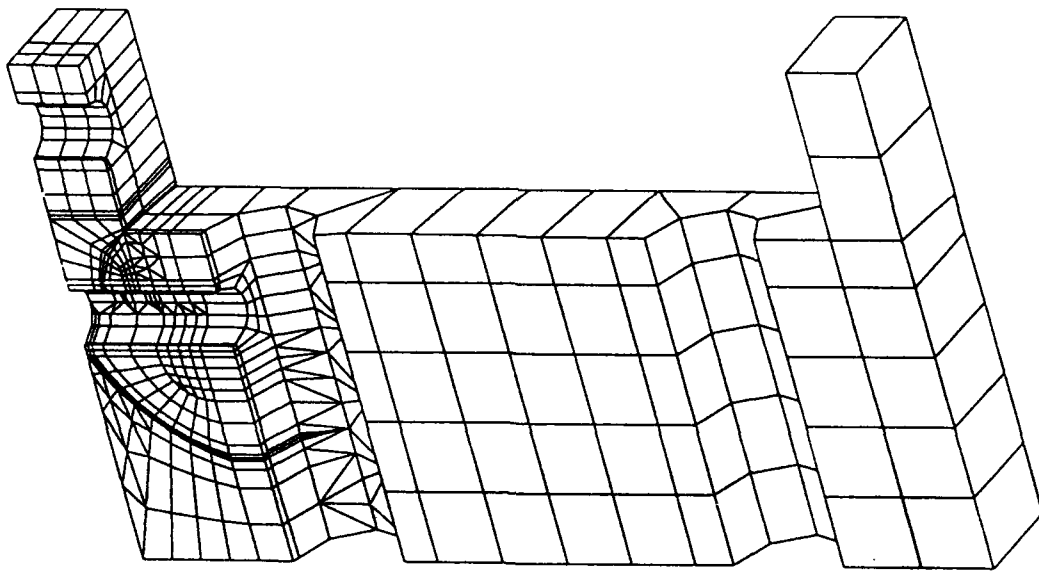


Figure 10 F.E. mesh for crack case 2

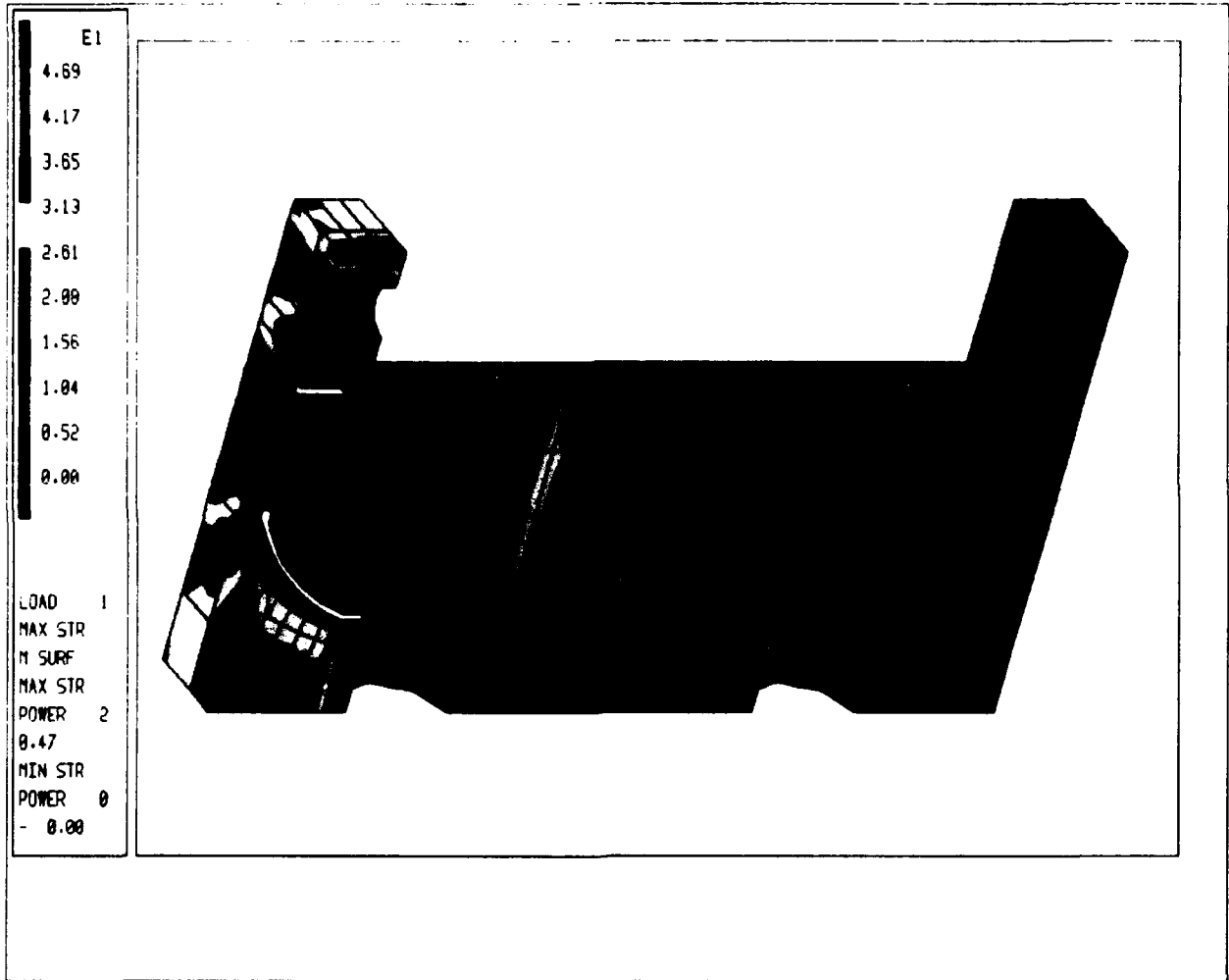


Figure 11 Maximum principal stress solution for crack case 2

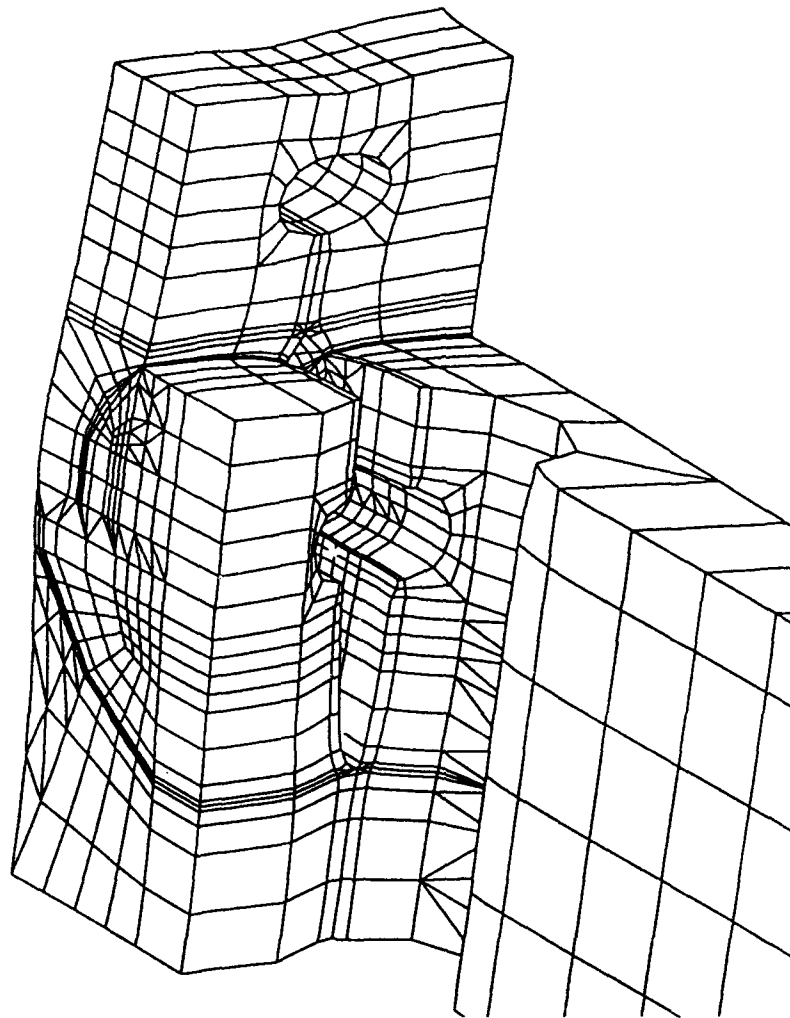
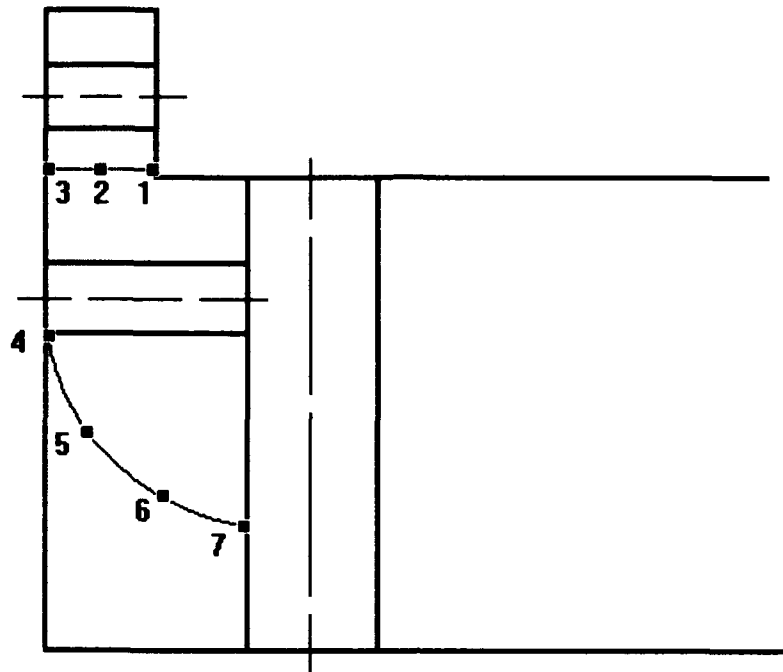


Figure 12 Displaced mesh for crack case 2



Location	K_I (MPa $\sqrt{m/g}$)
1	3.10
2	3.38
3	3.14
4	4.90
5	2.85
6	2.52
7	3.47

Figure 13 Stress intensity factors for case 2.

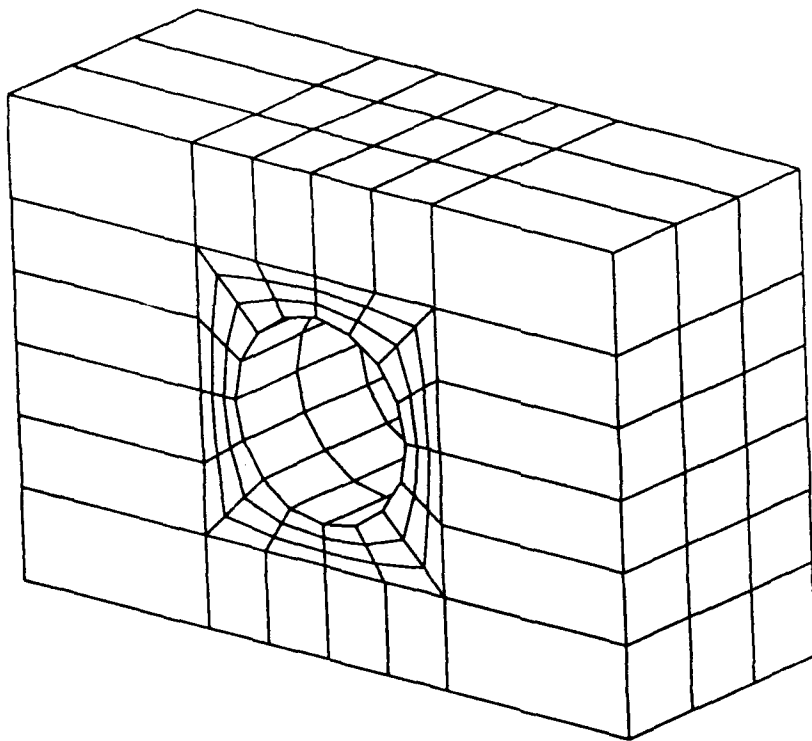


Figure 14 F.E. mesh for plastic analysis of hole D15

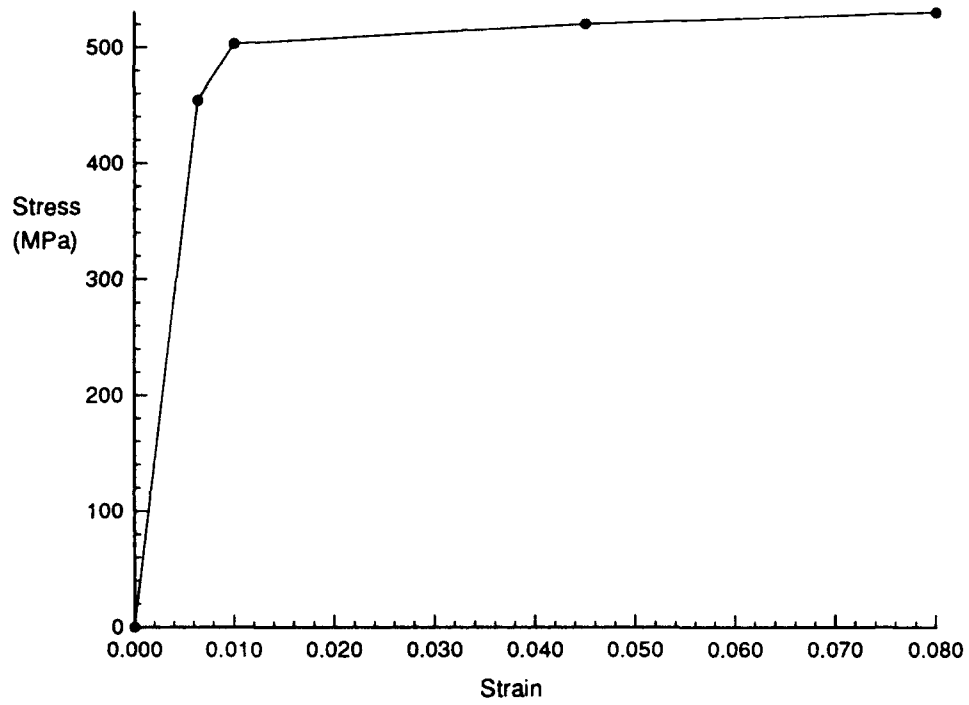


Figure 15 Approximation of stress-strain curve for *Al 7075*

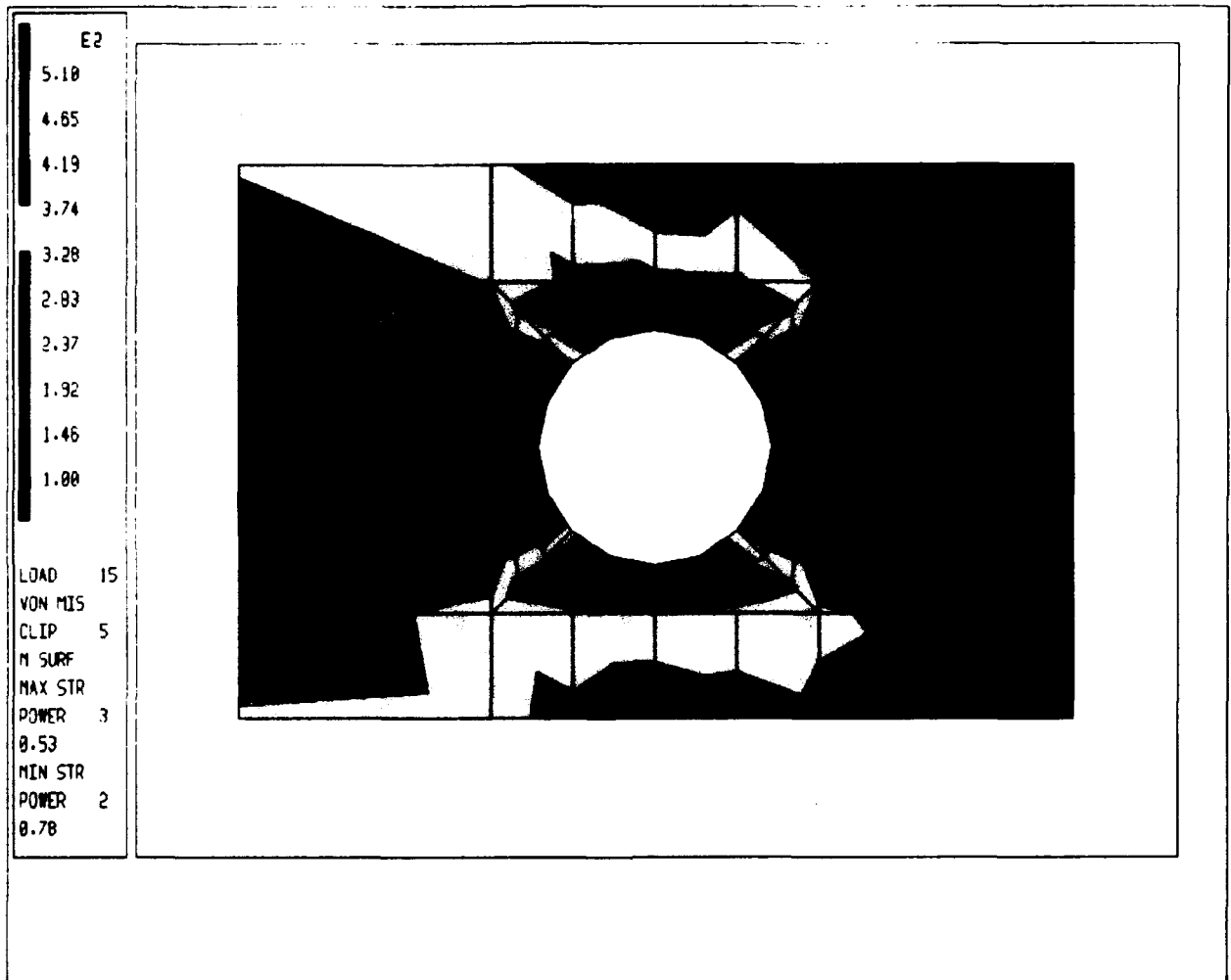


Figure 16 Plastic solution (von Mises stress) of the flange hole for the uncracked case

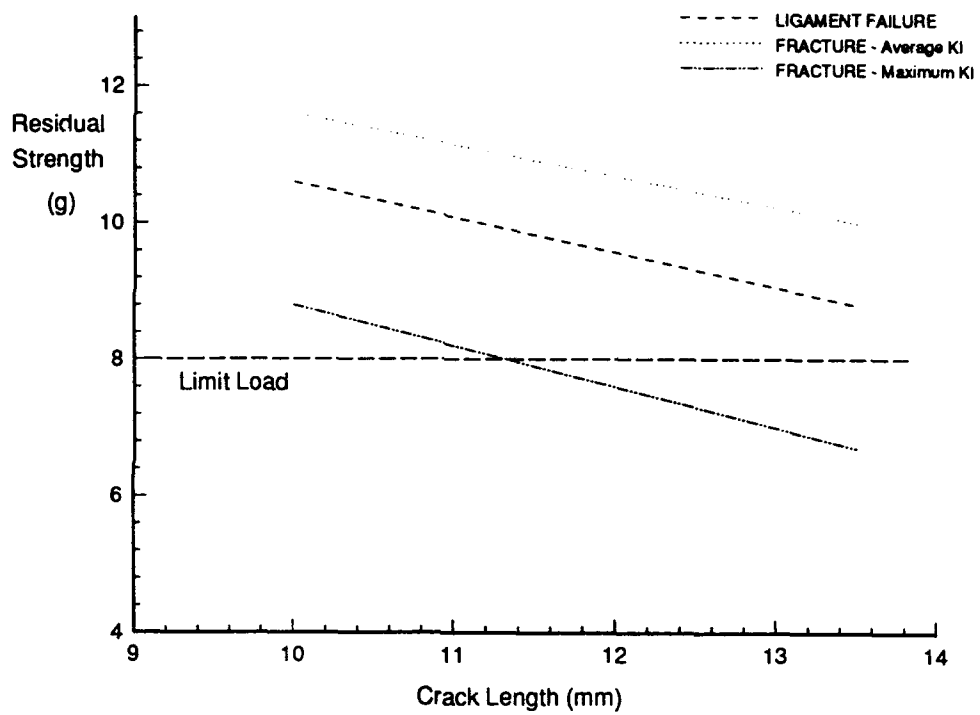


Figure 17 Residual strength vs crack length

DISTRIBUTION

AUSTRALIA

DEFENCE ORGANISATION

Defence Science and Technology Organisation

Chief Defence Scientist
FAS Science Policy
AS Science Corporate Management } shared copy
Counsellor Defence Science, London (Doc Data Sheet only)
Counsellor Defence Science, Washington (Doc Data Sheet only)
Senior Defence Scientific Adviser (Doc Data Sheet only)
Scientific Advisor Policy and Command (Doc Data Sheet only)
Navy Scientific Adviser (3 copies Doc Data Sheet only)
Scientific Adviser - Army (Doc Data Sheet only)
Air Force Scientific Adviser
Scientific Adviser to Thailand MRD (Doc Data sheet only)
Scientific Adviser to the DRC (Kuala Lumpur) (Doc Data sheet only)

Aeronautical Research Laboratory

Director
Library
Chief Airframes and Engines Division
Author: D. Rees
G. Jost
M. Heller
J. Paul
R. Kaye
T. Van Blaricum
G. Clark

Defence Central

OIC TRS, Defence Central Library
Document Exchange Centre, DSTIC (8 copies)
Defence Intelligence Organisation
Library, Defence Signals Directorate (Doc Data Sheet Only)

HQ ADF

Director General Force Development (Air)

Air Force

Aircraft Research and Development Unit
Scientific Flight Group
Library
PDR AF
DENGPP-AF
AHQ (SMAINTSO)
DGELS AIRREG4 HQLC
OIC ATF, ATS, RAAFSTT, WAGGA (2 copies)

OTHER

Australian Defence Force Academy
Library
Head of Aerospace and Mechanical Engineering
AGPS
NASA (Canberra)

SPARES (6 COPIES)
TOTAL (41 COPIES)

DOCUMENT CONTROL DATA

PAGE CLASSIFICATION
UNCLASSIFIED

PRIVACY MARKING

1a. AIR NUMBER AR-008-410	1b. ESTABLISHMENT NUMBER ARL-TN-63	2. DOCUMENT DATE DECEMBER 1993	3. TASK NUMBER AIR 92/054
4. TITLE FINITE ELEMENT ANALYSIS OF MB326H MACCHI WING LOWER SPAR CAP FATIGUE CRACKS		5. SECURITY CLASSIFICATION (PLACE APPROPRIATE CLASSIFICATION IN BOX(S) RE. SECRET (S), CONF. (C) RESTRICTED (R), LIMITED (L), UNCLASSIFIED (U)).	
		6. NO. PAGES 25	
8. AUTHOR(S) D. REES		9. DOWNGRADING/DELIMITING INSTRUCTIONS Not applicable.	
10. CORPORATE AUTHOR AND ADDRESS AERONAUTICAL RESEARCH LABORATORY AIRFRAMES AND ENGINES DIVISION 506 LORIMER STREET FISHERMENS BEND VIC 3207		11. OFFICE/POSITION RESPONSIBLE FOR: RAAF DAIRREG SPONSOR _____ SECURITY _____ DOWNGRADING _____ APPROVAL _____ CAED	
12. SECONDARY DISTRIBUTION (OF THIS DOCUMENT) Approved for public release. OVERSEAS ENQUIRIES OUTSIDE STATED LIMITATIONS SHOULD BE REFERRED THROUGH DSTIC, ADMINISTRATIVE SERVICES BRANCH, DEPARTMENT OF DEFENCE, ANZAC PARK WEST OFFICES, ACT 2601			
13a. THIS DOCUMENT MAY BE ANNOUNCED IN CATALOGUES AND AWARENESS SERVICES AVAILABLE TO No limitations			
13b. CITATION FOR OTHER PURPOSES (RE. CASUAL ANNOUNCEMENT) MAY BE			
		<input checked="" type="checkbox"/> UNRESTRICTED OR	<input type="checkbox"/> AS FOR 13a.
14. DESCRIPTORS Cracking (fracturing) Stress intensity factors Macchi MB326H aircraft Wing spars		Holes (openings) Finite element analysis	
		15. DISCAT SUBJECT CATEGORIES 201101 0103	
16. ABSTRACT <i>A three dimensional finite element analysis of cracks in the MB326H Macchi wing lower spar cap is presented. The case of cracks emanating from the intersection of a wing attachment fitting bolt hole and a web attachment fastener hole at wing station Y900 is considered. Stress intensity factors for two proposed crack geometries and the residual strength of the ligament above the web attachment fastener hole in the spar cap flange are calculated.</i>			

PAGE CLASSIFICATION
UNCLASSIFIED

PRIVACY MARKING

THIS PAGE IS TO BE USED TO RECORD INFORMATION WHICH IS REQUIRED BY THE ESTABLISHMENT FOR ITS OWN USE BUT WHICH WILL NOT BE ADDED TO THE DISSEMINATED DATA UNLESS SPECIFICALLY REQUESTED.

16. ABSTRACT (CONT).

17. IMPRINT

AERONAUTICAL RESEARCH LABORATORY, MELBOURNE

18. DOCUMENT SERIES AND NUMBER

Technical Note 63

19. WA NUMBER

24 226F

20. TYPE OF REPORT AND PERIOD COVERED

21. COMPUTER PROGRAMS USED

22. ESTABLISHMENT FILE REF.(S)

23. ADDITIONAL INFORMATION (AS REQUIRED)